

Cite this: *J. Mater. Chem. A*, 2015, 3, 1110

Novel morpholinium-functionalized anion-exchange PBI–polymer blends

Carlo Gottardo Morandi,^a Retha Peach,^b Henning M. Krieg^b and Jochen Kerres^{*ab}

Novel morpholinium-functionalized anion-exchange blend membranes are presented in this study. The blended membranes consist of highly brominated poly(aryl ether) (PAE-Br) or poly(2,6-dimethyl-1,4-phenyleneoxide) (PPO-Br), partially fluorinated polybenzimidazole (F₆-PBI) as the polymer matrix and/or a sulfonated polyethersulfone from 1,1'-biphenyl-4,4'-diol and potassium 5,5'-sulfonylbis(2-fluorobenzenesulfonate), abbreviated in this study as SAC. One of the manufactured blend membranes (IEC: 2.4 mmol g⁻¹) had a better alkaline stability than the Tokuyama membrane A201. In addition, excellent thermal stability and moderate water uptake were observed for the blend. The enhanced thermophysical properties were ascribed to the PBI matrix, whereas the high bromination degree of the ionomer contributed to the high ion-exchange capacities and conductivities obtained. The significantly increased chemical stability noted for these blends can partially be attributed to supplementary ionic cross-links formed between acidic and basic components. These results, combined with the ability of PPO-Br and PAE-Br to form macroscopically homogeneous blends with PBIs, resulting in stable and flexible polymer films, reiterate the potential suitability of the presented membranes as polymer electrolytes for electrochemical applications such as alkaline fuel cells.

Received 23rd September 2014
Accepted 6th November 2014

DOI: 10.1039/c4ta05026f

www.rsc.org/MaterialsA

1 Introduction

It is a matter of fact that an environmentally aware use of energy is one of the most critical challenges of the future. Among all renewable energy technologies, the fuel cell is a promising field, once a fuel cell is a power unit that directly converts chemical into electrical energy, heat and water by means of a redox reaction.^{1–5} Since the fuel cell is not subjected to the limitations of a Carnot cycle, high efficiencies can be attained.

Currently, much interest is being directed towards the research of alkaline anion-exchange membrane based fuel cells (AEMFCs), which turned out to be an alternative technology that can overcome the cost and technological barriers of proton-exchange membrane fuel cells (PEMFCs). By partially replacing platinum with cheaper non-noble metal catalysts and avoiding the use of Nafion® or similar polymers, which are often used in PEMFCs, a potentially improved price–performance ratio can be obtained.⁶

In an attempt to minimize the carbonation problem in alkaline media, anionic polymer membranes have been developed, also within this study, as electrolytes. The AEM plays an essential role in AEMFCs, as it serves as a barrier between the fuel and the oxidant while also supporting the catalyst. To date,

there is no AEM commercially available which is at the same time chemically, mechanically and thermally stable, while maintaining high conductivities. This is generally due to the poor chemical stability of AEMs in alkaline media.^{7,8} In order to overcome these obstacles, we present within this study the use of ionic cross-linking between the alkaline anion exchange polymer and minor amounts of a sulfonic aromatic compound (SAC) as an approach to further enhance the alkaline stability of the AEMs by formation of acid–base polymer cross-linking, whereas the addition of the inert polymer compound F₆PBI, referred to as the polymer matrix, increases the AEM mechanical stability by formation of polymer blends, *i.e.*, membranes which consist of a mixture of polymers. These polymers are depicted in Fig. 1.

The search for suitable anion exchange ionomers as starting polymers for the preparation of novel AEMs is still in its early stages of development. Exchange-active groups are normally introduced to the polymer structure by means of a halomethylation reaction. This reaction is a Friedel–Crafts alkylation which has various disadvantages, including (i) the reaction is not well controllable and often yields a randomly cross-linked product,⁹ (ii) the control of the electrophilic substitution position is non-specific and can occur from the side chain to the polymer backbone, (iii) the reaction is not always reproducible,^{9–12} and (iv) halomethyl methyl ethers are particularly dangerous carcinogens and must be synthesized or used in closed systems.¹³ In agreement with that, this study focused on the direct bromination of a partially fluorinated

^aInstitute of Chemical Process Engineering, University of Stuttgart, D-70199, Stuttgart, Germany. E-mail: jochen.kerres@icvt.uni-stuttgart.de

^bFocus Area: Chemical Resource Beneficiation Faculty of Natural Science, North-West University, Potchefstroom 2520, South Africa

studied for fuel cell applications²⁷ as well as “pure” PBI-based membranes – doped with KOH – used in alkaline H₂ (ref. 28) and direct alcohol fuel cells.²⁹ Chromik *et al.* (2013)³⁸ showed that polybenzimidazoles, such as the partially fluorinated polybenzimidazole (F₆PBI), are suitable as matrix polymers to markedly enhance not only the mechanical but also thermal properties of ionomers. Even though the addition of an inert blend component or a supporting structure to anion-exchange ionomers leads to a drop in the conductivity, non-supported anion-exchange ionomers usually lack mechanical strength if their ion-exchange capacities (IECs) are set high for sufficient anion-conductivity (IEC > 2 meq. OH⁻ per g). Within this work, this could be confirmed in the course of preliminary tests: non-supported binary ionically cross-linked blends from the anion exchange polymer and SAC, with a calculated IEC of 2.2 meq. g⁻¹, showed good ion conductivities, but were extremely brittle.

This study presents the synthesis of morpholinium-type anion-exchange polymers, which were obtained by the reaction of the bromomethyl groups of a bromomethylated polymer with the tertiary amine *N*-methylmorpholine (represented in Fig. 3) and further combination with minor amounts of a sulfonated polymeric aromatic compound (SAC). SAC was applied as a macromolecular ionic cross-linker. The sulfonic acid groups of the SAC component interact with the nitrogen base of either F₆PBI or quaternized *N*-methylmorpholine (NMM) by protonation of the basic N atom, resulting in polysalts with interchain ionic cross-linking (Fig. 4). The ionic cross-links promoted by

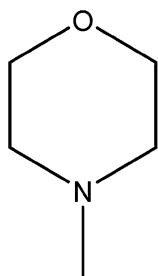


Fig. 3 Chemical structure of *N*-methylmorpholine.

the introduction of SAC can be ascribed to polysalt formation with both the PBI-matrix and the quaternized polymer.

Additionally, the bromomethylated backbone polymers PPO-Br and PAE-Br (for structures, see Fig. 2) used in this study were further covalently cross-linked by either adding the diamines DABCO or TMEDA to the polymeric solution. The respective chemical structures are depicted in Fig. 5. In the literature it is also common to make use of an external cross-linker such as divinylbenzene (DVB) for covalent cross-linking, but this was not the scope of this study. For quaternization purposes, morpholine was used to yield a morpholinium-functionalized blend membrane. In the literature, quaternary ammonium salts (QA) are often reported as cationic groups. A variety of mono- and diamines have already been investigated for quaternization focusing mainly on trimethylamine (TMA)^{30–32} and DABCO.^{8,33–36} The latter is chemically more stable than other diamines, while achieving high membrane conductivities. In turn, NMM has not been widely investigated yet; Hahn *et al.* (2013)³⁷ synthesized a morpholinium-functionalized poly(ether sulfone) *via* polycondensation followed by methylation of the polymer-pendent morpholine group. However, this AEM reported a relatively low hydroxide conductivity of 16 mS cm⁻¹ at RT (IEC: 0.9 meq. g⁻¹) (Fig. 6).

Within the framework of this study, novel acid–base blend AEMs were developed and characterized in terms of their thermophysical and electrochemical properties, *e.g.* anion-exchange capacity, ion conductivity, weight loss after extraction with solvent, water uptake, and alkaline stability. Based on the

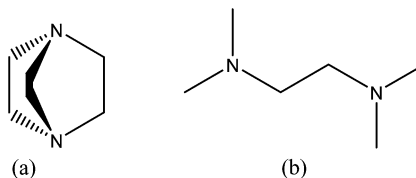


Fig. 5 Chemical structures of the diamines (a) DABCO and (b) TMEDA for additional superficial covalent cross-linking within the polymer blend.

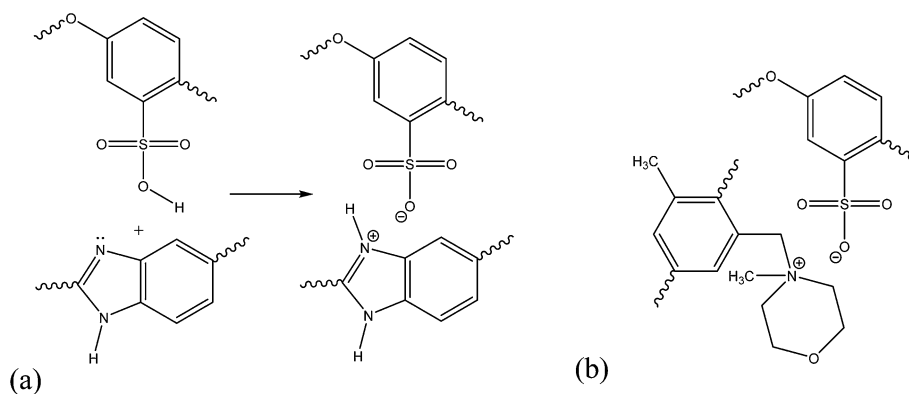


Fig. 4 Ionic cross-linking between the sulfonic aromatic compound (SAC) and (a) partially fluorinated imidazole (F₆PBI) by imidazole group protonation or (b) by quaternization with *N*-methylmorpholine. SAC is added in minor amounts as a third blend component to enhance the chemical stability by formation of ionic cross-links.

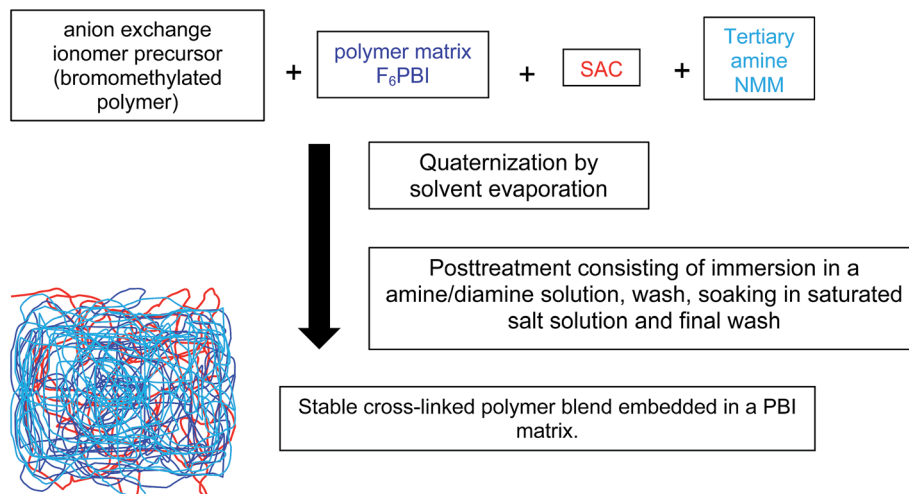


Fig. 6 Membrane preparation and post-treatment.

results, a parallel was drawn between the two different backbone polymers PPO-Br and PAE-Br analyzed. In addition, different compositions and quaternization approaches were investigated while studying the influence of covalent and ionic cross-linking on the alkaline stability. For comparative purposes the Tokuyama membrane A201 was included in the study. The main objective of this work was to find an AEM, which is mechanically, thermally, and chemically stable while being OH-conductive in alkaline media.

2 Experimental

2.1 Materials

All chemicals were used as received without any further purification steps. Poly(2,6-dimethyl-1,4-phenylene oxide) (PPO) was obtained from General Electric Plastics. *N*-Bromosuccinimide (NBS), 1,4-diazabicyclo[2.2.2]octane (DABCO), chlorobenzene, *N,N*-dimethylacetamide (DMAc), 4,4'-isopropylidenebis(2,6-dimethylphenol) (TMBP), anhydrous *N*-methyl-2-pyrrolidone (NMP), 4-methylmorpholine and *N,N,N',N'*-tetramethylethylenediamine (TMEDA) were purchased from Sigma Aldrich. Azobis(isobutyronitrile) (AIBN) was purchased from Merck, F₆PBI from YANJIN Technology, 305 International Enterprises Center, 2 Huatian Road, Huayuan Industrial Park, Tianjin 300384, CHINA. Decafluorobiphenyl (DFBP) was obtained from ABCR, analytical chloroform from Carl Roth GmbH, while deuterated chloroform from Deutero GmbH. Ethanol was purchased from VWR International. SAC was prepared within this research group by the polycondensation of 1,1'-biphenyl-4,4'-diol with 4,4'-sulfonylbis(fluorobenzene) (50 mol%) and potassium 5,5'-sulfonylbis(2-fluorobenzenesulfonate) (50 mol%).³⁸ Membrane A201 from Tokuyama was used as received.

2.2 Bromination of PPO

For bromination the NBS method previously developed within this research group was used.¹⁴

2.2.1 Synthesis and bromination of PAE. The method previously developed within this research group for the synthesis of PAE and following bromination¹⁴ was used as described in Fig. 2. 80 mmol of tetramethyl-bisphenol A (TMBP, chemical name 4,4'-(propane-2,2-diyl)bis(2,6-dimethylphenol)), 80.6 mmol of decafluorobiphenyl (DFBP) and 480 mmol of potassium carbonate were added to 360 ml of anhydrous *N*-methyl-2-pyrrolidone (NMP) under an argon atmosphere. The polymer solution was heated to 80 °C. After 24 hours, the reaction mixture was cooled to room temperature. The solution was precipitated in 1.5 l of water. The precipitated polymer was filtered off and washed repeatedly with hot water. Finally the polymer was dried at 90 °C.

Yield: 41.5 g (71.74 mmol, 89.7%).

To brominate PAE to PAE-Br, 12 mmol of partially fluorinated PAE were dissolved in 120 ml of chloroform. Subsequently, 97 mmol of NBS and 0.1 mmol of BPO (radical initiator, for generation of Br[•] radicals) were added to the reaction solution, which was heated to 61 °C. The temperature was held constant for 24 hours. Finally, the reaction mixture was cooled to room temperature and the brominated polymer was precipitated into 0.5 l of methanol. The precipitated polymer was filtered off and washed several times using hot methanol, before it was dried at 90 °C.

Yield: 10.3 mmol (85.2%); substitution degree: 81.2%.

¹H NMR CDCl₃, ppm, 250 Hz: δ = 7.19 (H-12); 7.05 (H-17); 6.92 (H-23, X = Br); 6.86 (H-23, X = H); 4.42 (H-11); 4.38 (H-19); 2.12 (H-22); 2.07 (d, 4J = 3.05 Hz, H-22, X = H); 1.75–1.55 (m, H-14); ¹³C NMR CDCl₃, 63 Hz, ppm: δ = 150.88 (C-9); 150.31 (C-20, X = H); 150.19 (C-20, X = Br); 148.94 (C-3, X = H); 148.34 (C-3, X = Br); 147.38 (C-6); 142.98 (C-16, X = H); 142.02 (C-16, X = Br); 141.72 (C-13); 138.10 (C-1, X = H); 137.82 (C-1, X = Br); 137.58 (C-8); 137.25 (C-7); 137.09 (C-7); 130.70 (C-12); 130.67 (C-23, X = Br); 130.27 (C-23, X = H); 130.19 (C-23, C-17, X = H); 130.07 (C-18, X = H); 129.98 (C-18, X = Br); 129.83 (C-21); 129.24 (C-10); 127.54 (C-17); 100.84 (C-4); 100.34 (C-5); 42.78 (C-15, X = Br); 42.58 (C-15, X = H); 30.66 (C-14); 26.80 (C-19, X = Br); 26.66

(C-11); 16.57 (C-22); ^{19}F NMR CDCl_3 , 235 Hz, ppm: δ -138.09 (F-6, F-3); -156.13 (F-7, F-2). Elemental analysis (% , experimental): C = 43.00; H = 2.30; F = 15.78; Br = 33.39. (% , calculated, 100% bromination): C = 41.64; H = 2.03; F = 17.00; Br = 35.75; O = 3.58. NMR assignments see Fig. 2.

2.2.2 Polymer matrix. PPO-Br or PAE-Br was blended with F_6PBI (Fig. 1), resulting in macroscopically homogeneous, stable and flexible polymer films. The unmixed synthesized PPO-Br was hydrophilic due to the high bromination degree achieved and did not form a mechanically stable AEM.

2.3 Membrane preparation

The polymer matrix (F_6PBI), the brominated polymer (PPO-Br and PAE-Br) and the sulfonated aromatic compound (SAC) were each dissolved in DMAc (5 wt% polymeric solutions). After combining and subsequently stirring the polymer solutions, NMM was added in a stoichiometric four-fold excess, so as to guarantee complete quaternization. Before mixing, both the polymer solutions and the NMM were cooled down to $-20\text{ }^\circ\text{C}$, in order to suppress possible premature cross-linkings, interactions and quaternization reactions. The polymer film was formed at $80\text{ }^\circ\text{C}$ for 12 h by solvent evaporation in a convection oven equipped with a leveled surface. The AEM was post-treated primarily by immersing the membrane in the appropriate amine solution for two days as specified in Table 1 to ensure 100% amination/quaternization and in the case of a diamine additional covalent cross-linking. Next, the membranes were soaked in distilled water at $90\text{ }^\circ\text{C}$ for two more days to remove the surplus amine solution and reaction remnants before being placed in a saturated sodium chloride solution for two days at $90\text{ }^\circ\text{C}$ to convert the membrane to the Cl^- form. Finally, the membranes were soaked in distilled water at $50\text{ }^\circ\text{C}$ to wash out the excess salt. The membrane preparation is schematized in Fig. 7. The membranes were stored in the chloride form to avoid carbonate formation, otherwise possible when the membranes are in the OH^- form.

The membranes synthesized with their respective compositions and post-treatments are listed in Table 1. The blend membranes will hereafter be referred to as in Table 1. The benchmark membrane Tokuyama A201 (development code: A006) was analyzed as a reference.

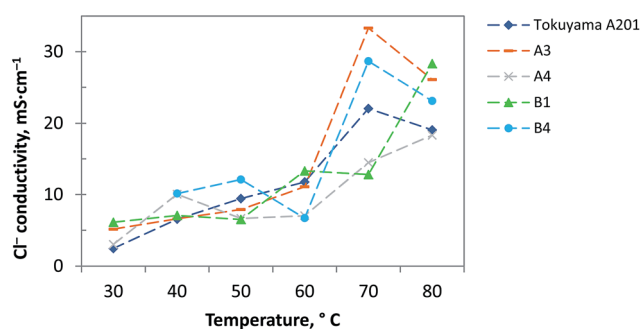


Fig. 7 Chloride conductivities at a RH of 90%.

2.4 Polymer characterization

2.4.1 Structure analysis. The bromination degree was determined by nuclear magnetic resonance (NMR) spectroscopy. Proton NMR (^1H NMR) spectra were obtained on a Bruker Avance 400 spectrometer with a resonance frequency of 500 MHz at $30\text{ }^\circ\text{C}$ using deuterated chloroform. In the ^1H NMR spectra, the various peaks were integrated and placed in relation to each other. By comparing the intensity of the H signals related to the methyl groups with that of the bromomethylene groups (CH_2Br), it was possible to calculate the bromination degree (eqn (1)).³⁹ The bromine content could be confirmed by elemental analysis.

$$\text{BD} [\%] = \frac{3I(\text{H} - \text{CH}_2\text{BR})}{3I(\text{H} - \text{CH}_2\text{BR}) + 2I(\text{H} - \text{CH}_3)} \times 100\% \quad (1)$$

BD = bromination degree; $I(\text{H} - \text{CH}_2\text{Br})$ = intensity of the H signal corresponding to bromomethylene groups; $I(\text{H} - \text{CH}_3)$ = intensity of the H signal corresponding to methyl groups.

2.5 Membrane characterization

2.5.1 Weight loss after extraction with solvent. In order to determine to what extent the AEMs dissolved in an organic solvent, extractions with DMAc were performed. Before extraction, the dry weight of the membranes in the Cl^- form was determined. Subsequently, the AEMs were soaked in DMAc at $80\text{ }^\circ\text{C}$ for four days to extract the non-cross-linked or easily soluble fractions of the membrane. After solvent extraction the membranes were soaked in distilled water for two days at $80\text{ }^\circ\text{C}$.

Table 1 Composition and post-treatment of synthesized anion-exchange blend membranes

Membrane	Backbone polymer [mg]	F_6PBI [mg]	SAC [mg]	NMM* [ml]	Post-treatment
A1	PPO-Br; 125	125	—	0.3	TMEDA, $80\text{ }^\circ\text{C}$
A2	PPO-Br; 202.5	202.5	20.25	0.59	TMEDA, $80\text{ }^\circ\text{C}$
A3	PPO-Br; 202.5	202.5	20.25	0.59	15% NMM in EtOH, $50\text{ }^\circ\text{C}$
A4	PPO-Br; 202.5	202.5	—	0.59	15% NMM in EtOH, $50\text{ }^\circ\text{C}$
B1	PPO-Br; 202.5	202.5	60.75	0.59	50% DABCO in EtOH, $50\text{ }^\circ\text{C}$
B2	PAE-Br; 243	162	20.25	0.45	50% DABCO in EtOH, $50\text{ }^\circ\text{C}$
B3	PAE-Br; 243	162	40.5	0.45	50% DABCO in EtOH, $50\text{ }^\circ\text{C}$
B4	PAE-Br; 243	162	60.75	0.45	50% DABCO in EtOH, $50\text{ }^\circ\text{C}$

Finally, the extracted membranes were dried at 80 °C. The weight loss after extraction was calculated, using eqn (2).

$$WL = \left(1 - \frac{m_{\text{after}}}{m_{\text{before}}}\right) \times 100\% \quad (2)$$

WL: weight loss after extraction (%); m_{before} : membrane dry weight before extraction (g); m_{after} : membrane dry weight after extraction (g).

2.5.2 Ion exchange capacity (IEC). The IEC describes the amount of ion-exchange groups per weight unit of the dry ion-exchange membrane in meq. g⁻¹ or mmol g⁻¹ for monovalent ions. Before IEC measurements, all AEMs were converted to the OH⁻ form by soaking the membrane samples in a 1 M potassium hydroxide solution for at least 4 h at 50 °C. Afterwards they were immersed in deionized water over an argon blanket for at least 4 h to remove the excessive hydroxide while avoiding the contact with air and changing the water occasionally. Subsequently, each AEM sample was immersed in 50 ml of a saturated sodium chloride solution for 24 h at 50 °C to replace all hydroxide counter-ions with chloride ions. Following this, 3 ml of a 0.1 N hydrochloric acid standard solution was added. After approximately 6 hours, the membrane sample was removed from the solution and thoroughly rinsed with water, which was added to the solution. The amount of exchanged hydroxide ions was determined by back-titration, using a 0.01 N sodium hydroxide standard solution. Before drying the membrane samples at 80 °C and weighing them in the Cl⁻ form, they were immersed in water for 12 h to remove the surplus sodium chloride. The OH⁻ weight was calculated on the basis of the Cl⁻ weight, so that the total IEC could be determined, using eqn (3).

$$IEC_{\text{total}} = \frac{C_{\text{HCl}} V_{\text{HCl}} - C_{\text{NaOH}} V_{\text{NaOH}}}{m_{\text{dry}}} \quad (3)$$

IEC_{total} = total ion-exchange capacity (mmol g⁻¹); C_{HCl} = concentration of the hydrochloric acid solution (M); C_{NaOH} = concentration of the sodium hydroxide solution (M); V_{HCl} = added volume of hydrochloric acid solution (L); V_{NaOH} = added volume of sodium hydroxide solution (L); m_{dry} = dry weight of the membrane sample in the OH⁻ form (g).

2.5.3 Water uptake (WU). For the determination of the water uptake, the membrane samples were dried at 50 °C under vacuum before weighing (m_{dry}). Subsequently, they were stored in deionized water, until equilibrium was reached at 30 °C. The weight of the wet membrane (m_{wet}) was measured after gently removing the surface water with absorbent paper. The water uptake of the membrane was calculated using eqn (4). All water uptake measurements were performed with membranes in the hydroxide/carbonate form.

$$WU [\%] = \left(\frac{m_{\text{wet}} - m_{\text{dry}}}{m_{\text{dry}}}\right) \times 100 \quad (4)$$

WU = water uptake; m_{wet} = wet weight of the membrane (g); m_{dry} = dry weight of the membrane (g).

2.5.4 Impedance and conductivity. A Solartron 1260 impedance spectrometer was used in the frequency range of 10–10⁶ Hz, in a typical through-plane four-electrode AC arrangement. The preconditioning time at 30 °C was set to one hour, to

ensure that equilibrium had been attained. The relative humidity was set to 90% and held constant during the experiment. The temperature was varied from 30 to 80 °C. At specific temperatures, a three-fold measurement was performed. A Nyquist plot was recorded and the ohmic resistance, derived from the high-frequency intercept of the complex impedance with the real axis, was obtained. Eqn (5) describes how the conductivity was calculated from the ohmic resistance and the resistivity therefrom.

$$\sigma = \frac{1}{R_{\text{sp}}} = \frac{d}{RA} \quad (5)$$

σ : conductivity [mS cm⁻¹]; R_{sp} : resistivity [Ω cm]; d : thickness of the membrane [cm]; R : ohmic resistance [Ω]; A : electrode dimensions [cm²].

The membranes were all stored in deionized water for at least 24 h before the measurement. Since it was not possible to avoid contact with air while sandwiching the membrane between the electrodes and mounting the cell, the chloride conductivity was measured. The membranes are stable in air in the chloride form but not in the hydroxide ion form due to the carbonation phenomenon ($\text{Q}^+\text{OH}^- + \text{CO}_2 \rightarrow \text{Q}^+\text{HCO}_3^-$). The ionic conductivity at infinite dilution of Cl⁻ is 76.3×10^{-4} m² S mol⁻¹, while OH⁻ ions have a 2.595-times higher conductivity under the same conditions.⁴⁰ HCO₃⁻, however, has a conductivity at infinite dilution of 44.5×10^{-4} m² S mol⁻¹, which is even lower than that of Cl⁻ ions.

To avoid the carbonation phenomenon and enable a relative comparison of the synthesized membranes regarding their electrochemical properties, chloride conductivities of the membranes in the fully hydrated state (in 1 M NaCl equilibrating solution) were also determined *via* impedance spectroscopy. A Zahner-elektrik IM6 impedance spectrometer was used in through-plane mode. The impedances were investigated in the frequency range of 200 kHz to 8 MHz (amplitude: 5 mV). A three-fold measurement was performed for each membrane sample.

2.5.5 Alkaline stability. In order to investigate the chemical stability of the AEMs in a basic environment, the membrane samples were immersed in a 1 M potassium hydroxide solution at 90 °C for 10 days (very harsh alkaline environment). Decreases in IEC and/or chloride conductivity due to the alkaline treatment were determined and compared to the corresponding untreated membrane samples.

2.5.6 Thermal stability. The thermal stability of the membranes in the chloride form was analyzed by thermogravimetry (TGA, Netzsch, model STA 499C) at a heating rate of 20 °C min⁻¹ under an O₂-enriched O₂/N₂ atmosphere (65–70% O₂). The outlet products were continuously investigated by TGA-FTIR coupling (Nicolet Nexus, FTIR spectrometer).

3 Results and discussion

3.1 Membrane characterization

All of the summarized data regarding the characterization of the membranes prepared within this study are summarized in Table 2. The results will be discussed in Sections 3.1.1 to 3.1.6.

Table 2 Summary of the characterization parameters of the synthesized AEMs^a

Membrane	WL [wt%]	IEC _{exp.} [mmol g ⁻¹]	WU 30 °C [wt%]	WU 80 °C [wt%]	Cl ⁻ σ , RT 1 M NaCl [mS cm ⁻¹]	Cl ⁻ σ , 30 °C RH = 90% [mS cm ⁻¹]	σ/σ_0 , 90 °C 240 h in 1 M KOH [%]	T_{onset} [°C]
A1	13.6	2.6	74	83	67	5.7	<4	n.a.
A2	n.a.	1.8	47	n.a.	5	n.a.	62	273
A3	5.0	2.4	65	76	17	5.2	n.a.	261
A4	n.a.	3.3	71	111	9	3.0	59	250
B1	11.9	2.6	108	n.a.	22	6.1	n.a.	263
B2	6.6	3.2	81	n.a.	11	n.a.	52	n.a.
B3	3.7	2.5	67	70	10	n.a.	58	232
B4	4.8	2.0	50	71	12	n.a.	43	n.a.
Tokuyama	5.4	1.7	19	n.a.	12	2.4	21	166

^a IEC = ion exchange capacity; σ = conductivity; σ/σ_0 = conductivity decrease; RH = relative humidity; WU = water uptake; WL = weight loss; T_{onset} = onset temperature of polymer backbone degradation; n.a. = not completed.

Note that, when the investigated membranes performed weaker in the preliminary characterizations, further measurements were limited. Therefore n.a. was assigned in Table 2 to some membranes.

3.1.1 Weight loss after extraction with solvent. Membrane A1, which was covalently cross-linked along its surface by post-treatment with TMEDA (di-quaternization), reported a weight loss of 13.6 wt% after extraction. Komkova *et al.* (2004)³⁵ studied many aliphatic diamines and observed that the degradation of the membranes depends on the length of the alkanolic chain in the diamine units, that is, a slower degradation rate can be assigned to membranes with longer alkanolic residue membranes. In the same study, TMEDA and bis-*N,N,N',N'*-tetramethylbutanediammonium (TMBDA) reported a significant degradation, while membranes containing *N,N,N',N'*-tetramethylhexanediammonium (TMHDA) were the most stable in alkaline media. Therefore, in this study, the decrease in alkaline stability noted in the presence of TMEDA in membrane A1, together with the absence of ionic cross-linking, may have contributed to the relatively large weight loss after extraction. Membrane B1, additionally, reported a weight loss of 11.9 wt%, which can be ascribed to the dissolution of the fixed ions in DMAc at 80 °C, which is supported by the high water uptake (108 wt%) at 30 °C. Membranes A3 and B2–B4 reported smaller weight losses after extraction, which were mainly attributed to supplementary ionic cross-links due to the presence of SAC.

3.1.2 Ion-exchange capacity. The experimental IEC of the covalent-ionically cross-linked membrane A2 was the lowest reported (1.8 mmol g⁻¹) of all the synthesized anion-exchange blend membranes (Table 2), with the exception of the Tokuyama reference membrane. A2's homologues membrane A1 reported an IEC of 2.6 mmol g⁻¹ in the absence of additional ionic cross-links. In view of this, the relatively low IEC reported for A1 was attributed to the tightening up of the polymeric network promoted by the strong covalent–ionic cross-links. In contrast, membranes A4 and B2 presented relatively high experimental IECs, likely due to the formation of covalent cross-links between the polybenzimidazole (PBI) matrix and PPO-Br when exposed to a temperature of 80 °C during solvent evaporation, provided that both N's of the PBI are alkylated by the

reaction with CH₂Br groups. This hypothesis was confirmed by supplementary IEC measurements of equivalent membrane compositions without NMM. For example, the NMM-absent equivalent membrane for B1, that is, strictly the same composition as B1 but lacking the amine (NMM), still reported an IEC of 1.2 mmol g⁻¹ (46% of the B1's IEC). This clearly indicates that also F₆PBI serves as a base and covalently cross-links with PPO-Br. Moreover, an increased reactivity can be expected in modified PBIs,⁴¹ thus leading to higher alkylation degrees and subsequently higher IECs. Additionally, it was also observed that a higher SAC content leads to lower IECs. Membrane B2 (5 wt% SAC) had an IEC of 3.2 mmol g⁻¹, compared to membrane B3 (10 wt% SAC) and B4 (15 wt% SAC) with IECs of 2.5 mmol g⁻¹ and 2.0 mmol g⁻¹, respectively (Table 2). This can be enlightened by the formation of ionic cross-links, as depicted in Fig. 4, which occur at the expense of the IEC.

3.1.3 Water uptake. At 30 °C all investigated membranes, except for B1, reported water uptake below 81 wt%. This is in agreement with literature values, which vary from 10 to 70 wt% at ambient temperatures.^{6,42} The commercially available Tokuyama membrane A201 reported a water uptake of merely 17 wt% at 30 °C which can be traced back to hydrophobic covalent cross-links being present in the Tokuyama membrane.⁴³ As a result of covalent as well as ionic cross-linking, a tightening within the polymer network can be assumed for membrane A2. This leads to a relatively low water uptake at RT (47 wt%). In contrast, due to the absence of ionic cross-links, membrane A4 reported a higher water uptake, reaching 111 wt% at 80 °C. In spite of the absence of ionic cross-linking, covalent cross-links between the bromomethylated polymer and the PBI matrix are believed to take place. It is well-known that non-cross-linked AEMs can report much higher water uptake, up to 300 wt% prior to membrane solubility.^{44,45} Finally, in spite of the covalent–ionic cross-linking, the high water uptake of membrane B1 can be assigned to the high localized concentrations of ionic groups and large hydration numbers promoted by the use of DABCO [compare Fig. 5].

3.1.4 Impedance and conductivity. For fuel cell application, conductivities of usually 10⁻¹ S cm are needed for high current density cell outputs.⁴⁶ Literature values of hydroxide

conductivities for AEMs (at RT and in distilled water) vary between 10^{-3} to 0.1 S cm^{-1} .⁶ The Tokuyama membrane A 201 (development code A 006) reports a hydroxide conductivity (RH = 90%) of 40 mS cm^{-1} (IEC: 1.7 meq. g^{-1})⁴⁷ at room temperature, and is considered the commercial AEM with the highest ion conductivity to date.

When fully hydrated and in the chloride form, a chloride conductivity (1 M NaCl, RT) of 12 mS cm^{-1} was obtained for the Tokuyama membrane A201 (Table 2) within this work. According to the results obtained for the membranes developed in this study, membranes A1 (67 mS cm^{-1}), A3 (17 mS cm^{-1}) and B1 (22 mS cm^{-1}) performed better than the commercial AEM, while membranes B2, B3 and B4 yielded chloride conductivities that were similar to that of the reference membrane.

In Fig. 7, the chloride conductivity measured for membranes A3, A4, B1, B4 and Tokuyama A201 in a humidified atmosphere (RH = 90%) is depicted as a function of the temperature. Membranes A1, A2, B2 and B3 were not further investigated in terms of chloride conductivity. A1 did not report good chemical stability, as it will be further discussed in Section 3.1.5, while A2 was not found suitable due to poor ion conductivity in 1 M NaCl. B4 can be considered representative for B2 and B3 due to similar compositions. At RT, all the presented membranes reported higher chloride conductivities in a humidified atmosphere (3.0 to 6.1 mS cm^{-1}) than that of the benchmark membrane (2.4 mS cm^{-1}). At higher temperatures, membranes A3, B1 and, to some extent, A4 had similar ion conductivities to the commercial membrane. From Fig. 7, it is also evident that the ion conductivity increased with increasing temperatures for all membranes. This was attributed to the increased water uptake reported at higher temperatures (Table 2), which favors the ion mobility due to the thermal expansion of the ion-transport channels.

3.1.5 Alkaline stability. The alkaline stability was evaluated either in terms of the decrease noted in ionic conductivities and/or IECs measured under harsh alkaline conditions. The ionic conductivities of the morpholinium-quaternized membranes are represented in Fig. 8. The benchmark membrane reported a poor chemical stability in alkaline media, with only 21% of the

initial conductivity retained after the stability test. In contrast to the commercial membrane, which also reported a significant color change at higher pHs, the presented membranes, with the exception of A1, still seemed mechanically stable after the alkaline treatment. This observation is supported by Fig. 8(a) and (b), wherein it is evident that both the ammonium groups and the polymer backbone of membranes A1 and Tokuyama A201 degraded significantly, confirmed by their decreased conductivities at a higher degradation rate (63–97% degradation after 240 h) compared to the respective ion-exchange groups (17–40% degradation after 240 h).

Membrane A1, which was covalently cross-linked with TMEDA, lost 97% of its conductivity after 120 h in KOH. This can be attributed to the use of TMEDA as a cross-linker and the lack of ionic cross-links (no addition of SAC). The use of TMEDA is believed to promote chain scission, as indicated in the recent literature³⁵ and explained earlier in this study, thus resulting in poor alkaline stabilities. The observed lack of stability could be solved either by adding SAC to ionically cross-link the membrane (membrane A2), or by excluding TMEDA in the post-treatment (membrane A4) or both (membrane A3). Of its original conductivity membrane A2 retained 82% after 120 h and 62% after 240 h of alkaline treatment. This verifies the effectiveness of the acid–base blend concept, where SAC contributes to an increased cohesion of the membrane. However, the increase in chemical stability occurred at the expense of the conductivity (Table 2) to some extent. For membrane A3, 59% of its ammonium groups remained intact after the alkaline treatment. Surprisingly, membrane A4 reported a relatively high conductivity after the alkaline treatment (59% of the original value). This could be ascribed to additional interactions resulting from the morpholine oxygen atom, thus compensating for the absence of cross-links. Finally, no clear conclusion could be drawn between the content of the sulfonated polymer (5, 10, and 15 wt%) and the alkaline stability.

3.1.6 Thermal stability. In order to compare the effects of the different polymers used within the blends, the separate components of the blended membranes were thermally investigated (Fig. 9). PPO-Br ($T_{\text{onset}} = 180 \text{ }^\circ\text{C}$) and PAE-Br ($T_{\text{onset}} = 175 \text{ }^\circ\text{C}$) had

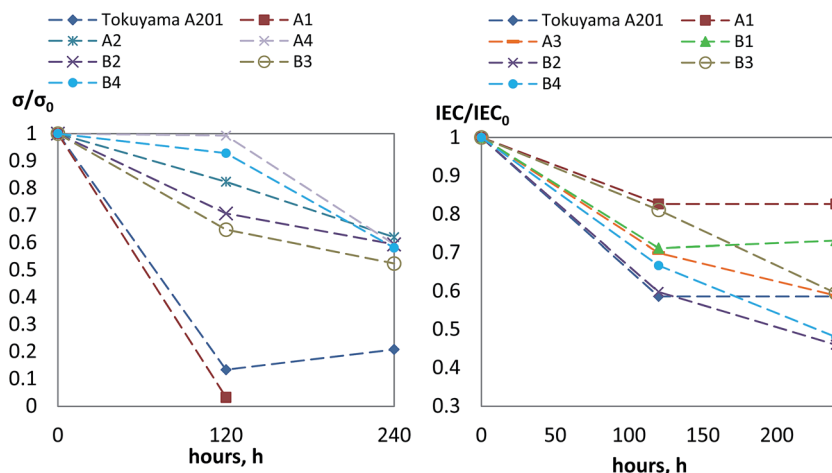


Fig. 8 (a) Conductivity and (b) IEC decrease in the course of an alkaline stability test (1 M KOH, 90 °C).

similar thermal stabilities, while F₆PBI was, as expected, much more stable in regards to the thermal resistance than the bromomethylated polymers, thereby contributing to the overall thermal stability of the polymer blend.

The thermal stabilities of selected membranes from this study are depicted in Fig. 10, showing that the synthesized membranes had excellent short-term thermal stabilities. However, it has to be noted that TGA serves as an indicator for short-term thermal stabilities in the fuel cell; long-term thermal stabilities cannot be assessed by means of TGA.

After amination, the hydrophilicity of the membranes increases, resulting in an increased water content compared to a non-functionalized polymer. This bounded water evaporated at 50–200 °C. For all the synthesized membranes, a second weight loss occurred after 230 °C. The lowest thermal stability was observed for the Tokuyama membrane, showing significant degradation beyond 167 °C, which can be ascribed to the decomposition of the ionomer backbone. This was verified by means of TGA-FTIR coupling, where vibrations of carbon monoxide observed at wavenumbers of 2300–2100 cm⁻¹ indicated aromatic degradation of the ionomer backbone. For the *T*_{onset} values of all the membranes thermally investigated, refer back to Table 2. Due to the inherent thermal stability of SAC, no

obvious effect on the overall thermal stability of the membrane could be observed.

4 Conclusions

Within this study, novel ionically cross-linked AEM blends comprising *N*-methylmorpholinium anion-exchange groups embedded in a stable PBI matrix were investigated. These blend membranes reported moderate water uptake (high enough to promote ion hydration and improve conductivity, but low enough to avoid excessive swelling and prevent poor mechanical stability). Relatively good chemical and thermal stabilities were also reported. Specifically, it was shown that the addition of polymeric acid (the sulfonated polyethersulfone, SAC) had a clear impact on the measured IEC. This was likely due to acid–base interactions within the blend: higher SAC contents in the acid–base blend led to lower IECs, with membrane B2 (5 wt% SAC) having an IEC of 3.2 mmol g⁻¹, while membrane B3 (10 wt%) had an IEC of 2.5 mmol g⁻¹ and B4 (15 wt% SAC) had 2.0 mmol g⁻¹. This implies that additional ionic cross-links were formed at the expense of the total amount of available ammonium groups. TMEDA as a post-treatment agent (di-quaternization of superficial remaining CH₂Br groups) was proven unstable in an alkaline environment, while the tertiary diamine DABCO, in combination with PPO-Br, resulted in higher water uptake of the resultant AEM blend membranes. The weight loss after extraction correlated to water uptake. At 30 °C, all investigated membranes, except for B1, reported water uptake below 81 wt%. Membrane A1 (covalently cross-linked with TMEDA) proved unstable in alkaline media, but its homologue membrane A2 (ionically cross-linked with SAC) retained 62% of its original conductivity after 240 h in a very harsh alkaline environment. The effectiveness of the ionic cross-linking was hereby verified, where SAC contributed to an increased cohesion of the membrane. In addition, all synthesized membranes had excellent short-term thermal stabilities (>230 °C), which could be traced back to both the chemically stable PBI matrix and the added sulfonated macromolecular ionic cross-linker SAC, in contrast to the membrane A201 from Tokuyama (*T*_{onset} = 167 °C).

While membrane B1 also reported positive results, the high water uptake (108 wt%) at 30 °C led to solvation of macro-ions during the extraction tests, contributing to a weight loss after solvent extraction of 11.9 wt%, which discredits membrane B1 for application in alkaline fuel cells.

According to the results, the ionically cross-linked blend membrane A3 is a promising candidate for alkaline fuel cell applications. Apart from relatively high chloride conductivities (17 mS cm⁻¹ in 1 M NaCl; 5.2 mS cm⁻¹ in RH = 90%), excellent short-term thermal (*T*_{onset} = 261 °C) and mechanical stabilities (WU_{80 °C} = 76 wt%) were observed. Its alkaline stability (59% of its original IEC after 240 hours in KOH at 90 °C) was also much higher than that of the Tokuyama membrane A201. Surprisingly, the blend membrane A4, which lacks ionic cross-links, was relatively stable, retaining 59% of its original conductivity after 240 h in KOH at 90 °C, while maintaining excellent thermal stability (*T*_{onset} = 250 °C), good mechanical properties

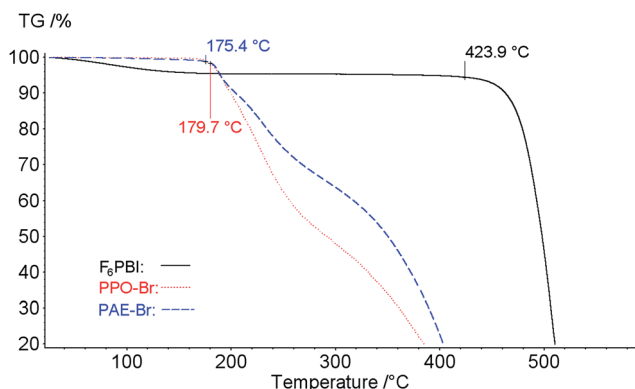


Fig. 9 TGA traces of the polymer components from the investigated AEMs at a heating rate of 1 °C min⁻¹.

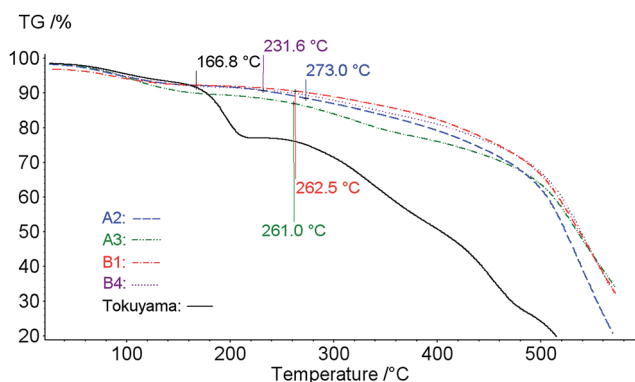


Fig. 10 TGA traces of selected anion-exchange blend membranes at a heating rate of 20 °C min⁻¹.

(WU_{30 °C} = 71 wt%) and a similar chloride conductivity to the commercial Tokuyama membrane A201.

The high thermal stability of F₆PBI, together with its ability to form macroscopically homogeneous polymer films with the brominated polymers, has qualified at least two of the developed polymer blends as promising candidates for fuel cell applications.

In future work, the R&D on ionically cross-linked blend AEMs will be continued. It is planned to investigate other combinations of the different blend components, including other PBIs, bromomethylated arylene main-chain polymers, tertiary amines and alkylated sterically hindered imidazoles with the objective to obtain novel AEM blends, which perform even better than the AEM blend systems reported in this study. First results on the use of alkylated imidazole compounds as quaternizing reagents showed promising results. In future work, the novel acid–base blend AEMs will be applied to alkaline fuel cells and electrolysis, including tailoring of electrodes for the novel AEM blend membrane concept.

Acknowledgements

The authors would like to thank the AiF-Bundesministerium für Wirtschaft und Technologie for the financial support within the project 402ZN/2. And the authors thank Inna Kharitonova and Galina Schumski for assistance on the polymer and membrane characterization.

References

- 1 L. Carrette, K. A. Friedrich and U. Stimming, Fuel cells – Fundamentals and Applications, in *Fuel Cells*, Wiley-VCH Verlag GmbH & Co. KGaA, Weinheim, 2001, pp. 5–39.
- 2 G. Hoogers, *Fuel Cell Technology Handbook*, CRC Press, Boca Raton, 2003.
- 3 J. Larminie and A. Dicks, *Fuel Cell Systems Explained*, J. Wiley, Chichester, 2nd edn, 2003, pp. 109–122.
- 4 R. Shah, Introduction to Fuel Cells, in *Recent trends in fuel cell science and technology*, ed. S. Basu, Springer, New York, 2007, pp. 1–9.
- 5 L. Gubler and G. G. Scherer, A Proton-Conducting Polymer Membrane as Solid Electrolyte – Function and Required Properties, in *Fuel Cells I*, ed. G. G. Scherer, Springer, Berlin, Heidelberg, 2008, pp. 1–14.
- 6 G. Merle, M. Wessling and K. Nijmeijer, *J. Membr. Sci.*, 2011, **377**, 1–35.
- 7 J. R. Varcoe and R. C. T. Slade, *Fuel Cells*, 2005, **5**(2), 187–200.
- 8 B. Bauer, H. Strathmann and F. Effenberger, *Desalination*, 1990, **79**, 125–144.
- 9 J. Zhou, M. Unlu, J. A. Vega and P. A. Kohl, *J. Power Sources*, 2009, **190**(2), 285–292.
- 10 G. Wang, Y. Weng, D. Chu, R. Chen and D. Xie, *J. Membr. Sci.*, 2009, **332**(1–2), 63–68.
- 11 M. R. Hibbs, M. A. Hickner, T. M. Alam, S. K. McIntyre, C. H. Fujimoto and C. J. Cornelius, *Chem. Mater.*, 2008, **20**(7), 2566–2573.
- 12 M. Tanaka, K. Fukasawa, E. Nishino, S. Yamaguchi, K. Yamada, H. Tanaka, B. Bae, K. Miyatake and M. Watanabe, *J. Am. Chem. Soc.*, 2011, **133**, 10646–10654.
- 13 Verordnung zum Schutz vor Gefahrstoffen, Gefahrstoffverordnung (Gefahrstoffverordnung – GefStoffV) 2010, last updated: 2013.
- 14 A. Katzfuß, Synthese und Charakterisierung von kovalent vernetzten Anionenaustauschermembranen und deren Einsatz in Direkt-Methanol-Brennstoffzellen, sowie ESR spektroskopische Messungen zur Identifikation der Radikalbildung in der Membran, Doctoral Dissertation, Universität Stuttgart, 2013, pp. 34–38.
- 15 W. I. Harris, Procédé de préparation de résines échangeuses d'anions à basse teneur en chlore, European Patent 0183158 A2, 1986.
- 16 W. F. H. Borman, Functional aromatic substituents in polyphenylene oxides, *US Pat.* 3226361, 1965.
- 17 P. Zschocke and D. Quellmalz, *J. Membr. Sci.*, 1985, **22**(2), 325–332.
- 18 K. Matsui, E. Tobita, K. Sugimoto, K. Kondo, T. Seita and A. Akimoto, *J. Appl. Polym. Sci.*, 1986, **32**(3), 4137–4143.
- 19 T. N. Danks, R. C. T. Slade and J. R. Varcoe, *J. Mater. Chem.*, 2003, **13**(4), 712–721.
- 20 G. Couture, A. Alaaeddine, F. Boschet and B. Ameduri, *Prog. Polym. Sci.*, 2011, **36**(11), 1521–1557.
- 21 B. Ameduri, *Chem. Rev.*, 2009, **109**(12), 6632–6686.
- 22 W. Offermann and F. Vögtle, *J. Org. Chem.*, 1979, **44**(5), 710–713.
- 23 C.-C. Huang, M.-S. Yang and M. Liang, *J. Polym. Sci., Part A: Polym. Chem.*, 2006, **44**(20), 5875–5886.
- 24 K. Miyatake, H. Zhou and M. Watanabe, *J. Polym. Sci., Part A: Polym. Chem.*, 2005, **43**(8), 1741–1744.
- 25 G. Cheney, M. E. Van Dyke and S. J. Clarson, *J. Inorg. Organomet. Polym. Mater.*, 1998, **8**(2), 119–126.
- 26 Y.-L. Liu, Y.-H. Chang and M. Liang, *Polymer*, 2008, **49**(25), 5405–5409.
- 27 J. Kerres, A. Ullrich, F. Meier and T. Häring, *Solid State Ionics*, 1999, **125**(1–4), 243–249.
- 28 O. Savadogo and B. Xing, *J. New Mater. Electrochem. Syst.*, 2000, **3**, 345–349.
- 29 H. Hou, G. Sun, R. He, B. Sun, W. Jin, H. Liu and Q. Xin, *Int. J. Hydrogen Energy*, 2008, **33**(23), 7172–7176.
- 30 J. R. Varcoe, *Phys. Chem. Chem. Phys.*, 2007, **9**(12), 1479–1486.
- 31 L. Wu and T. Xu, *J. Membr. Sci.*, 2008, **322**(2), 286–292.
- 32 M. R. Hibbs, C. H. Fujimoto and C. J. Cornelius, *Macromolecules*, 2009, **42**(21), 8316–8321.
- 33 M. Faraj, E. Elia, M. Boccia, A. Filpi, A. Pucci and F. Ciardelli, *J. Polym. Sci., Part A: Polym. Chem.*, 2011, **49**, 3437–3447.
- 34 J. Wang, G. He, X. Wu, X. Yan, Y. Zhang, Y. Wang and L. Du, *J. Membr. Sci.*, 2014, **459**, 86–95.
- 35 E. Komkova, D. Stamatialis, H. Strathmann and M. Wessling, *J. Membr. Sci.*, 2004, **244**(1–2), 25–34.
- 36 T. Sata, M. Tsujimoto, K. Yamaguchi and T. Matsusaki, *J. Membr. Sci.*, 1996, **112**, 161–170.
- 37 S. J. Hahn, M. Won and T. H. Kim, *Polym. Bull.*, 2013, **70**(12), 3373–3385.

- 38 A. Chromik and J. Kerres, *Solid State Ionics*, 2013, **252**, 140–151.
- 39 M. A. Al-Saleh, S. Gijltekin, A. S. Al-Zakri and H. Celiker, *J. Appl. Electrochem.*, 1993, **24**, 575–580.
- 40 P. Vanysek, Electrochemical series, in *CRC Handbook of Chemistry and Physics*, ed. D. R. Lide, CRC Press, pp. 5–95, 2004.
- 41 M. Hu, E. M. Pearce and T. K. Kwei, *J. Polym. Sci., Part A: Polym. Chem.*, 1993, **31**(2), 553–561.
- 42 G. Couture, A. Alaaeddine, F. Boschet and B. Ameduri, *Prog. Polym. Sci.*, 2011, **36**(11), 1521–1557.
- 43 Y. S. Li, T. S. Zhao and W. W. Yang, *Int. J. Hydrogen Energy*, 2010, **35**(11), 5656–5665.
- 44 K. M. Lee, R. Wycisk, M. Litt and P. N. Pintauro, *J. Membr. Sci.*, 2011, **383**(1–2), 254–261.
- 45 L. Sun, J. Guo, J. Zhou, Q. Xu, D. Chu and R. Chen, *J. Power Sources*, 2012, **202**, 70–77.
- 46 J. R. Varcoe, P. Atanassov, D. R. Dekel, A. M. Herring, M. A. Hickner, P. A. Kohl, A. R. Kucernak, W. E. Mustain, K. Nijmeijer, K. Scott, T. Xu and L. Zhuang, *Energy Environ. Sci.*, 2014, **7**(10), 3135–3191.
- 47 H. Yanagi and K. Fukuta, *ECS Trans.*, 2008, **16**(2), 257–262.